

Deleted: drought

1 **Expression of the “4.2 ka event” in the southern Rocky**
2 **Mountains, USA**

3

4

5 David T. Liefert¹, Bryan N. Shuman¹

6 1) Department of Geology and Geophysics, University of Wyoming, Laramie, WY 82070, USA

7

8

9

10

11

12

13

14

15

16

17

18

19

20

21

22

23

24 *Correspondence to:* David T. Liefert (dliefert@openspace.org)

26 **Abstract**

27 The use of the climatic anomaly known as the “4.2 ka event” as the stratigraphic division
28 between the mid- and late Holocene has prompted debate over its impact, geographic pattern,
29 and significance. The anomaly has primarily been described as abrupt drying in the Northern
30 Hemisphere at ca. 4 ka (ka, thousands of years before present), but evidence of the hydroclimate
31 change is inconsistent among sites, both globally and within North America. Climate records
32 from the southern Rocky Mountains demonstrate the challenge with diagnosing the extent and
33 severity of the anomaly. Dune-field chronologies and a pollen record in southeast Wyoming
34 reveal several centuries of low moisture at around 4.2 ka and prominent low stands in lakes in
35 Colorado suggest the drought was unique amid Holocene variability, but detailed carbonate
36 oxygen isotope ($\delta^{18}\text{O}_{\text{carb}}$) records from Colorado do not record drought at the same time. We find
37 new evidence from $\delta^{18}\text{O}_{\text{carb}}$ in a small mountain lake in southeast Wyoming of an abrupt
38 reduction in effective moisture or snowpack from approximately 4.2–4 ka, which coincides in
39 time with the other evidence of regional drying from the southern Rocky Mountains and the
40 western Great Plains. We find that the $\delta^{18}\text{O}_{\text{carb}}$ in our record may reflect cool-season inputs into
41 the lake, which do not appear to track the strong enrichment of heavy oxygen by evaporation
42 during summer months today. The modern relationship differs from some widely applied
43 conceptual models of lake-isotope systems and may indicate reduced winter precipitation rather
44 than enhanced evaporation at ca. 4.2 ka. Inconsistencies among the North American records,
45 particularly in $\delta^{18}\text{O}_{\text{carb}}$ trends, thus show that site-specific factors can prevent identification of the
46 patterns of multi-century drought. However, the prominence of the drought at ca. 4 ka among a
47 growing number of sites in the North American interior suggests it was a regionally substantial
48 climate event amid other Holocene variability.

Deleted: at ca. 4 ka

Deleted: it

51 **1. Introduction**

52 Rapid climate changes are well documented in the late Pleistocene and early Holocene,
53 such as during the Younger Dryas chronozone (ca. 12.9-11.7 ka, thousands of years before
54 present) and at 8.2 ka (Alley et al., 1997; Clark et al., 1999; Von Grafenstein et al., 1998), but
55 mid- to late-Holocene changes are less well understood (Wanner et al., 2008, 2011). One
56 potential abrupt change during this time, a multi-century climatic anomaly known as the “4.2 ka
57 event,” has been used as the benchmark for the stratigraphic division between the mid- and late
58 Holocene (Walker et al., 2019). Consequently, the 4.2 ka event has become a topic of scrutiny
59 with debate over its impact, geographic pattern, and significance (Bradley & Bakke, 2019;
60 Weiss, 2016, 2019). The ostensibly global event has primarily been described as a dry episode at
61 low and mid-latitudes (Booth et al., 2005; Nakamura et al., 2016; Di Rita & Magri, 2019;
62 Scuderi et al., 2019; Xiao et al., 2018). However, some regions show increased precipitation
63 (Huang et al., 2011; Railsback et al., 2018) or no change (Roland et al., 2014), as is consistent
64 with spatial variation expected from climate variability that shifts atmospheric waves and
65 dynamics.

66 The 4.2 ka event has been widely examined, but its cause and significance amid other
67 millennial-to-centennial climate variability during the Holocene remain unknown. Processes that
68 may have been involved in the event included changes in solar irradiance (Wang et al., 2005),
69 centennial-scale atmospheric circulations (Deininger et al., 2017), and latitudinal shifts in the
70 Intertropical Convergence Zone (Tan et al., 2008). Recent model simulations have produced
71 similar patterns of extended drought in the northern hemisphere without external forcings such as
72 insolation changes or volcanism (Yan & Liu, 2019), and others confirm that multi-decadal
73 megadroughts can arise through internal climate variability without changes in boundary

Moved (insertion) [1]

Deleted: s

Deleted: C

Deleted: , however,

Moved up [1]: some regions show increased precipitation (Huang et al., 2011; Railsback et al., 2018) or no change (Roland et al., 2014)

Deleted: R

81 conditions (Ault et al., 2018). Internal climate dynamics and feedbacks could also interact with
82 stochastic variability and external forcing to produce such events without consistent or linear
83 relationships to the forcing; forcing may only have a modest probability of triggering rapid
84 climate changes (Renssen et al., 2006). Less clear is how unusual or frequent prolonged
85 ‘megadroughts’ may be within the Holocene across different regions.

86 That such droughts can occur stochastically indicates the 4.2 ka event could be an
87 example of typical late-Holocene climate variability at multi-century time scales (Shuman &
88 Burrell, 2017), even if the event was exceptional within the spectrum of Holocene variability in
89 some regions. For example, the event is recorded in the northeastern United States as one
90 drought period within a series of Holocene wetting and drying events (Newby et al., 2014;
91 Shuman et al., 2019; Shuman & Burrell, 2017); evidence for a major hydroclimate change at ca.
92 4 ka has been growing in the North American midcontinent (Booth et al., 2005; Carter et al.,
93 2018; Dean, 1997; Denniston et al., 1992; Halfen & Johnson, 2013; Jiménez-Moreno et al.,
94 2019). ~~However, the event’s significance or uniqueness has been difficult to verify in this region~~
95 ~~because few sites document the anomaly compared to other regions of the mid-latitudes globally~~
96 (Ran & Chen, 2019; Zhang et al., 2018).

97 Records from the southern Rocky Mountains ~~of North America~~ demonstrate the
98 challenge. In the mid-latitude Rocky Mountains, only dune-field chronology and pollen records
99 have been explicitly interpreted to show the 4.2 ka event ~~while other record types, such as stable~~
100 ~~isotopes, have not~~. Initial recognition in North America derived from the timing of the
101 reactivation of the Ferris, Seminoe, and Casper Dune Fields in ~~southeast~~ Wyoming (Fig. 1, ~~Table~~
102 ~~1~~; Booth et al., 2005; Halfen et al., 2010; Stokes & Gaylord, 1993), but the extent of the drought
103 has been unclear because other dune-field chronologies in the adjacent western Great Plains do

Deleted: T

Deleted: , however,

Deleted: -central

107 not clearly document the drought (Dean, 1997; Halfen & Johnson, 2013; Mason et al., 1997).
108 More recently, Carter et al. (2013, 2017a, 2018) used fossil pollen from Long Lake in the
109 Medicine Bow Mountains, south of the Wyoming dune fields (Fig. 1, [Table 1](#)), to identify a 150-
110 year interval of increased temperature and decreased precipitation centered at 4.2 ka. The
111 inferred precipitation reductions were largest in springtime (Carter et al., 2018), when snowfall
112 in the southern Rocky Mountains is highest today (Mock, 1996). Consistent with this
113 interpretation, stratigraphic evidence of lake-level changes in Colorado and Wyoming lakes
114 could indicate that low-water phases at ca. 4.2 ka were one of the most prominent hydrologic
115 changes during the Holocene (Jiménez-Moreno et al., 2019; Shuman et al., 2009; Shuman et al.,
116 2014, 2015). [The drying event](#) stands out as one of the only multi-centennial features in a
117 summary of low lakes in the Rocky Mountains during the late-Quaternary (Shuman and
118 Serravezza 2017).

119 By contrast, the 4.2 ka event does not appear in stable oxygen isotope records from lakes
120 in the same region, such as detailed carbonate- $\delta^{18}\text{O}$ ($\delta^{18}\text{O}_{\text{carb}}$) records from Bison and Yellow
121 lakes, Colorado (Fig. 1, [Table 1](#); Anderson, 2011, 2012). Widely applied conceptual models of
122 lake-isotope systems indicate that [climate-driven changes in the stable isotope composition of](#)
123 [lake water become archived in lacustrine carbonates \(e.g., Anderson et al., 2016; Leng &](#)
124 [Marshall, 2004; Talbot, 1990\)](#). According to such models, [site-specific](#) hydrologic controls on
125 isotope budgets and the timing of carbonate formation should [also](#) play an important role in how
126 the [4.2 ka](#) event was recorded, but [the isotopic response should vary predictably by hydrologic](#)
127 [setting; long lake-water residence times and high evaporation cause hydrologically closed lakes](#)
128 (i.e., terminal basins) to record shifts in effective moisture (precipitation – evaporation) because
129 endogenic carbonates typically precipitate in evaporated, ^{18}O -rich water during the warm

Deleted: prominent

Deleted:

Deleted: It

Deleted: that

Deleted: (e.g., Anderson et al., 2016; Leng & Marshall, 2004; Talbot, 1990)

Deleted: rates of

Deleted: will

138 summer months. Drought could drive a positive change in the isotope composition of lake water
139 within such a lake-isotope system by both increasing evaporation and changing seasonal
140 precipitation, such as by reducing snowpack. In hydrologically open lakes with short residence
141 times, the continual replacement of evaporated water creates isotopic sensitivity primarily to the
142 seasonal balance of precipitation without a strong evaporation effect. In either model, $\delta^{18}\text{O}_{\text{carb}}$
143 tracks the isotope composition of lake water and its response to climate changes.

Deleted: affect

144 Many lakes fall somewhere between fully hydrologically open and closed and additional
145 site-specific influences may also override such expectations. Consequently, not all stable oxygen
146 isotope records from lakes may have been sensitive to the specific climate variables that changed
147 at 4.2 ka. Modern lake-water isotopic measurements (Fig. 2) can help to identify the relative
148 influences of different controls on the magnitude and range of lake-water $\delta^{18}\text{O}$, such as
149 groundwater fluxes and other seasonal dynamics that modify lake-water residence times. We
150 examine how the seasonality of carbonate formation could cause the relationships of lake-water
151 $\delta^{18}\text{O}$ to $^{18}\text{O}_{\text{carb}}$ to differ from the modern patterns observable in lakes today.

Deleted:

Deleted: (Fig. 2; Anderson et al., 2016)

152 Here we present a new $\delta^{18}\text{O}_{\text{carb}}$ record from Highway 130 Lake (HL) in southeast
153 Wyoming near where other Holocene paleohydrological and paleoecological records have been
154 developed (Fig. 1, Table 1; Mensing et al., 2012; Minckley et al., 2012; Brunelle et al., 2013).
155 HL is an intermittently closed subalpine lake in the Medicine Bow Mountains, within 20 km of
156 Long Lake where fossil pollen indicates a prolonged ‘megadrought’ at 4.2 ka (Carter et al.,
157 2018). The lake is also <60 km from Upper Big Creek Lake, Colorado, where a prominent
158 paleoshoreline detected in geophysical surveys and cores indicates low water after 4.7 ka (Fig. 1,
159 Table 1; Shuman et al., 2015). Previous work at HL indicates a strong influence of evaporation
160 on the lake and the stable isotope composition of its water, which we compare with Bison and

Deleted: Fig. 1;

Deleted: isotopes

166 Yellow lakes in Colorado (Fig. 2; Liefert et al., 2018). We discuss how dissimilarities in $\delta^{18}\text{O}_{\text{carb}}$
 167 among lakes, possibly driven by non-climatic factors, could complicate interpretations of the
 168 patterns of past hydroclimate changes including megadroughts and Holocene trends. Together
 169 these outcomes may clarify the timescales on which drought operates within a critical headwater
 170 area of North America, but also confirm that interpretations of past hydroclimate changes using
 171 $\delta^{18}\text{O}_{\text{carb}}$ may depend heavily on site-specific dynamics.

Deleted: of stable isotope records

173 **Table 1.** Changes at ca. 4.2 ka inferred from North American climate records nearby Highway
 174 130 Lake, southeast Wyoming, USA.

Study	Site Name	Region	Climate Record	Change at ca. 4.2 ka
Carter et al., 2013; 2017a	Long Lake	Southeast Wyoming, USA	Fossil pollen	Warming/drying
Halfen et al., 2010	Casper Dune Field	Southeast Wyoming, USA	Dune-field chronology	Drying
Stokes & Gaylord, 1993	Ferris/Seminole Dune Field	Southeast Wyoming, USA	Dune-field chronology	Drying
Anderson, 2011	Bison Lake	East-central Colorado, USA	Lacustrine carbonate $\delta^{18}\text{O}$	No prominent change
Anderson, 2012	Yellow Lake	East-central Colorado, USA	Lacustrine carbonate $\delta^{18}\text{O}$	No prominent change
Shuman et al., 2015	Upper Big Creek Lake	North-central Colorado, USA	Sedimentary lake-level record	Drying
Shuman et al., 2009a	Little Molas Lake	Central Colorado, USA	Sedimentary lake-level record	Drying
Shuman et al., 2014	Emerald Lake	Central Colorado, USA	Sedimentary lake-level record	Drying

175

176

178 2. **Site description**

179 HL (41°21'05" N, 106°15'50" W; 3,199 m a.s.l. (above sea level)) fills a shallow
180 depression in the uneven terrain covering the Libby Creek watershed (12 km² surface area) in the
181 Snowy Range, a southwest trending subsection of the Medicine Bow Mountains in southeast
182 Wyoming (Fig. 1). Around HL, subalpine coniferous forests interspersed with open meadows
183 grow on thin glaciated soils and tills between the frequent outcroppings of the underlying
184 siliceous metadolomite (Houston & Karlstrom, 1992; Musselman et al., 1992). Southeast
185 Wyoming has a semi-arid climate, but the Medicine Bow Mountains receive about 1,000 mm of
186 precipitation each year, with approximately 70% of annual totals falling as snow from October to
187 June (Mock, 1996). Local average wind speeds are high (~5 m/s) and minimum winter and
188 maximum summer temperatures typically reach -23°C and 21°C, respectively ([SNOTEL station](#)
189 [ID 367](#)).

190 The surface watershed around HL occupies ~0.45 km², while the lake has a surface area
191 of ~0.02 km², a maximum (spring) water depth of ~200 cm, and declines in water level by ~30
192 cm from July to late October (Liefert et al., 2018). Ice covers HL from approximately October to
193 May and stream connections shut off in June following spring flooding. Measurements reveal no
194 thermal stratification because of the shallow water depth, flat-bottom bathymetry, and high
195 average wind speeds, which promote mixing throughout the water column (Bello & Smith, 1990;
196 Stewart & Rouse, 1976). Liefert et al. (2018) found that evaporation could account for as much
197 as 83% of the seasonal water loss at HL, though the stable water level and temperature compared
198 to nearby lakes of similar size and depth indicates shallow groundwater flow-through driven by
199 seasonal precipitation and infiltration (Rautio & Korkka-Niemi, 2011; Rosenberry & LaBaugh,
200 2008).

Deleted: high elevations in

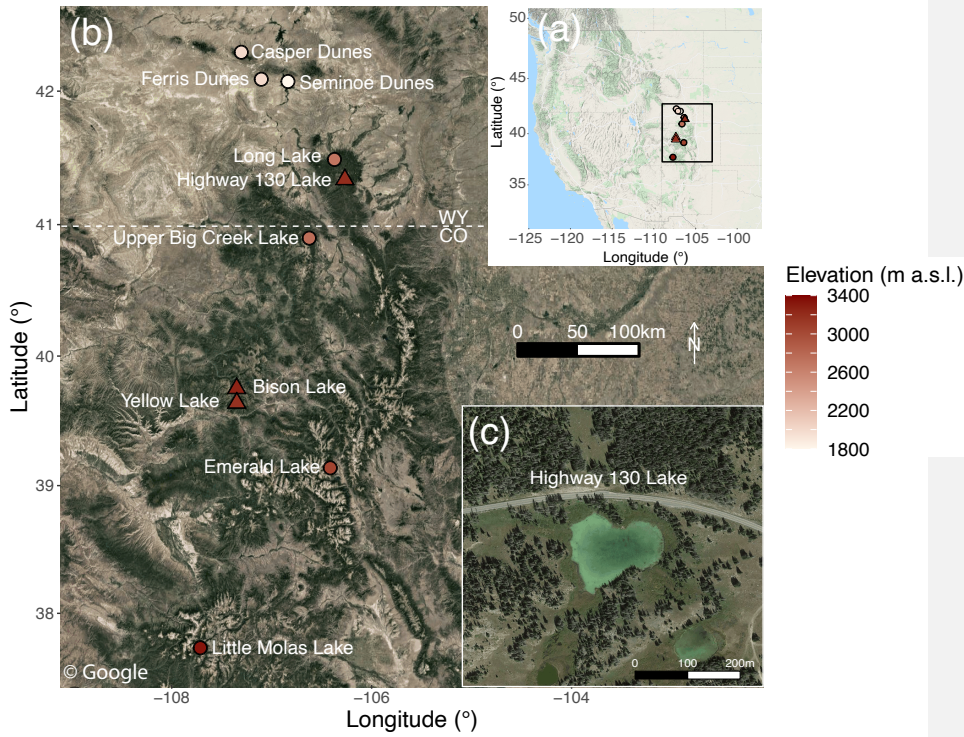


Figure 1. Locations of study site and related climate records. (a), Highway 130 Lake (triangle; **this study**) and related **carbonate (triangles), dune-field chronology, pollen, and lake-level** records (circles) lie within the southern Rocky Mountains, a critical headwater area in the western United States that contributes snowmelt to the Colorado and North Platte Rivers. (b), Study site locations in the Colorado Front Range and Medicine Bow Mountains, southeast Wyoming. (c), Highway 130 Lake lies within the Snowy Range, a subsection of the Medicine Bow Mountains. Google images (© Google Maps 2021) were acquired using the ggmap package in R (Kahle & Wickham, 2013).

Deleted: climate

Deleted: Little Molas Lake, a comparator site in the inset map (a), lies south of the focal region (b)

204 3. **Methods**

205 To measure the modern oxygen and hydrogen isotope compositions of the lake water
206 ($\delta^{18}\text{O}$ and δD , respectively), ~~temperature, and~~ specific conductance, water samples were
207 collected at approximately biweekly intervals from June to October, ~~in each year from 2015–~~
208 2017. Additional samples of snowfall, snowpack, rain, and groundwater (from springs and wells)
209 were collected ~~episodically from 2015–2017~~ to measure the range in water isotope values of the
210 watershed's hydrologic components. Isotopic ratios ~~of all water samples~~ were measured at the
211 University of Wyoming Stable Isotope Facility using a Picarro L2130-I Cavity Ring Down
212 Spectrometer and specific conductance was measured using a YSI Multiparameter Water Quality
213 Meter. ~~We report $\delta^{18}\text{O}$ and δD in the per mil (‰) notation relative to Vienna Standard Mean~~
214 ~~Ocean Water (VSMOW).~~ We acquired meteorological data from SNOTEL stations near HL at
215 Brooklyn Lake, Wyoming (ID 367; 3,121 m a.s.l.; 41.36 °N, -106.23 °W), and at Bison Lake,
216 Colorado (ID 345; 3,316 m a.s.l.; 39.76 °N, -107.36 °W), to compare the modern ratios of
217 snow/rain that control the seasonal balance of precipitation at the lakes.

218 In October 2016 we installed a pressure transducer (Onset HOBO U20 Level Data
219 Logger) to measure the water level ~~and temperature~~ of HL at 30-min intervals; freezing
220 conditions required that we secure the transducer to the lakebed inside a bladder filled with
221 antifreeze. To compensate for barometric pressure changes we adjusted the transducer data using
222 pressure measurements from the nearby Glacier Lakes Ecosystem Experiments Site Brooklyn
223 Tower Ameriflux site (GLEES Tower; US-GLE: <https://ameriflux.lbl.gov/sites/siteinfo/US-GLE>;
224 41°21'57" N, 106°14'23" W; 3,191 m a.s.l.). In late January 2017, we installed a conductivity
225 data logger (Onset HOBO U24 Conductivity Data Logger) at the same location and water depth
226 as the pressure transducer to measure the range in conductivity (converted to specific

Deleted: and

Deleted: in

229 conductance at 25 °C) at 30-min intervals of the unfrozen water underlying the ice cover to
230 examine the seasonal patterns of water chemistry that influence carbonate formation.

231 ~~On the same day in January 2017,~~ we collected a 70-mm diameter sediment core with a
232 modified Livingston piston corer from the center of HL where the combined water and ice depth
233 reached approximately 90 cm; we used this depth to calibrate the pressure transducer. The
234 organic and carbonate content of contiguous 1-cm intervals of the sediment core were measured
235 by weighing the residual sediment after burning the samples at 550 and 1000 °C, respectively.

236 ~~After the 550 °C burn removed organic matter, we isolated one-cm³ sub-samples from each~~
237 ~~interval for isotopic analysis; $\delta^{18}\text{O}_{\text{carb}}$ of samples burned were within the range of instrument~~
238 ~~uncertainty ($\pm 0.2\text{‰}$) as those with organic removal using oxidizing agents (typically bleach),~~
239 ~~indicating no additional fractionation.~~ Each sub-sample was sieved using a 63- μm mesh to
240 isolate the fine fraction ~~to be used~~ for isotopic analysis using a Thermo Gasbench coupled to a
241 Thermo Delta Plus XL isotope ratio mass spectrometer at the University of Wyoming Stable
242 Isotope Facility. X-ray powder diffraction (XRD) confirmed that the samples contained only
243 ~~microcrystalline calcite. We assume the calcite is predominantly autochthonous because the~~
244 ~~underlying metadolomite likely provides the Ca ions needed for carbonate formation (if the~~
245 ~~lacustrine carbonates were clastic deposits from metadolomite then its erosion should deposit~~
246 ~~more dolomite than calcite) and evidence of biogenic calcite within the core is rare (ostracod~~
247 ~~tests were present in less than 10 of the 300 samples).~~ We report $\delta^{18}\text{O}_{\text{carb}}$ in the per mil (‰)
248 notation relative to the Vienna Pee Dee Belemnite (VPDB) standard. ~~To calculate the~~
249 ~~temperature-dependent fractionation for calcite formation and convert from VSMOW to VPDB,~~
250 ~~we use equations from Leng and Marshall (2004).~~

Deleted: At the same time

Deleted: One-cm³ sub-samples were isolated from each interval ... a

Deleted: a

Deleted: burn

Deleted: to remove organic matter

Deleted: comparison

Deleted: ed

Deleted: were also sieved

Deleted: . O

Deleted: .

263 We isolated sedimentary charcoal (>125 μm) from the sediment core for radiocarbon
264 analyses to estimate sedimentation rates. Radiocarbon samples were analyzed at the University
265 of California Irvine Keck Carbon Cycle facility. We calibrated the radiocarbon chronology to
266 calendar years using intcal13 (Reimer et al., 2013) and generated the age-depth model and
267 uncertainties using Bchron (Parnell et al., 2008) and geoChronR (McKay et al., 2021).

Deleted: and conifer needles

Moved (insertion) [5]

Deleted: and

Deleted: was generated

Moved up [5]: Radiocarbon samples were analyzed at the University of California Irvine Keck Carbon Cycle facility.

269 4. Results

270 4.1 Modern water-chemistry and level measurements

271 Lake-water $\delta^{18}\text{O}$ and δD in HL increased during the ice-free season from -17.8‰ and -
272 132‰ (sampled in late June) to -10.8‰ and -94.2‰ (sampled in late October), respectively

273 (black circles, Fig. 2). The slope of the line tracing the seasonal range in HL's lake-water

Deleted: local evaporation line (LEL) defined

274 isotopes (thick black line, Fig. 2) traces the local evaporation line (LEL) defined by samples

Deleted: by the

Deleted: samples

275 from lakes in the Colorado Front Range (red dashed line, Fig. 2; Henderson & Shuman, 2009).

Deleted: LEL

276 Several consecutive years of measurements reveal that water isotope values at HL are consistent

277 from year to year. The LEL's deviation from both the global meteoric water line (GMWL; Fig.

278 2) and isotope composition of the hydrologic inputs (open symbols, Fig. 2) indicates a strong

279 evaporative influence. $\delta^{18}\text{O}$ and δD values at HL also indicate stronger fractionation by

280 evaporation compared to representative warm-season isotope compositions measured at Bison

281 and Yellow lakes from June–September around 2010 (thick purple and yellow lines, Fig. 2;

282 Anderson, 2011, 2012), which remained closer to the composition of meteoric waters. Longer

283 lake-water residence time and higher evaporation in HL thus appear to produce a greater range of

284 warm-season isotope compositions compared to Bison and Yellow Lakes.

294 The different lake-water- $\delta^{18}\text{O}$ values among the lakes contrasts with their similar
295 seasonal precipitation patterns. The modern ratio of snow/rain, which can determine the mean
296 precipitation and lake-water $\delta^{18}\text{O}$, is comparable in the watersheds of HL and Bison Lake [when](#)
297 [averaged from 1980–2019](#) (inset plot, Fig. 2). Other modern differences among the lakes, which
298 all have surface areas of $< 0.1 \text{ km}^2$, include that the maximum water depth of HL is several
299 meters shallower than Bison and Yellow Lakes (Anderson, 2012) and that the summer lake-
300 water temperatures in HL typically range from 8–12 °C, which is cooler than the epilimnion at
301 Yellow Lake (Anderson, 2012). HL is also several degrees cooler than nearby lakes also without
302 thermal stratification (Liefert et al., 2018).

303 Continuous measurements of specific conductance began in early February when the
304 combined water and ice depth reached approximately 90 cm (Fig. 3). Specific conductance
305 increased from 700 $\mu\text{S}/\text{cm}$ to 1,115 $\mu\text{S}/\text{cm}$ by early April while the lake surface was frozen. The
306 specific conductance fell below 500 $\mu\text{S}/\text{cm}$ as the lake flooded with snowmelt in early May.
307 Specific conductance ranged from 250–300 $\mu\text{S}/\text{cm}$ after the conductivity data logger was
308 removed in late June and before the lake froze over in the fall, and the water depth stayed
309 between 100–150 cm, which was low compared to previous years ([Liefert et al., 2018](#)).

310

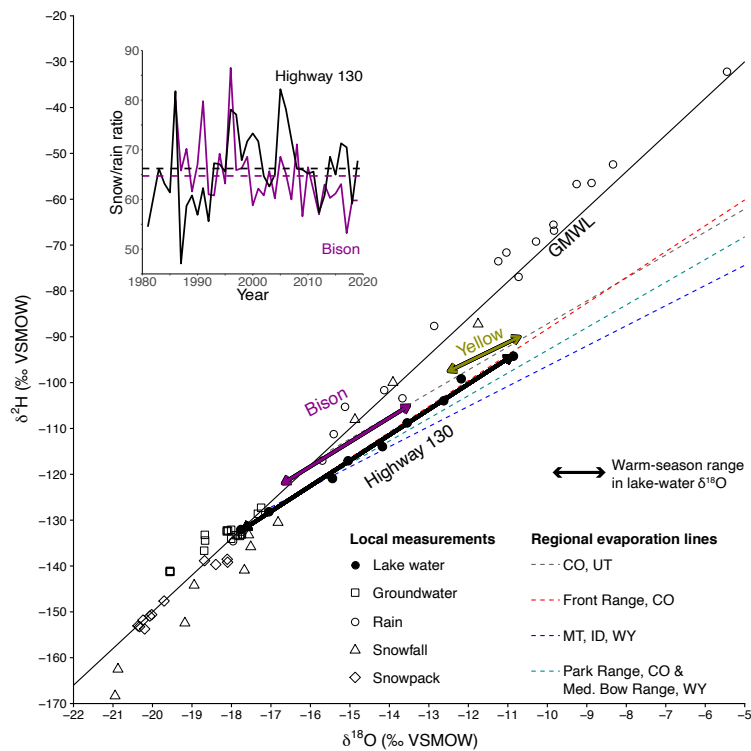


Figure 2. Modern measurements of $\delta^{18}\text{O}$ and δD . Samples from the study watershed shown here were collected throughout 2017. Regional evaporation lines (dashed lines; [Henderson & Shuman, 2009](#); [Anderson et al., 2016](#)) intersect the global meteoric water line and represent the linear regression of lake-water isotope compositions in a region. Isotopic measurements from the study watershed (open symbols) show the range in isotope compositions of hydrologic inputs to Highway 130 Lake from the watershed. Arrows represent the range in modern $\delta^{18}\text{O}$ and δD values of Highway 130 Lake (black), Bison Lake (purple; Anderson, 2011), and Yellow Lake (yellow; Anderson, 2012) throughout the ice-free season, and black dots show the individual measurements at Highway 130 Lake. The inset plot shows the modern annual ratio of snow/rain for the SNOTEL stations nearest Highway 130 Lake (black line) and Bison Lake (purple line) and the dashed lines show the means.

Deleted: (Henderson & Shuman, 2009; Anderson et al., 2016)...

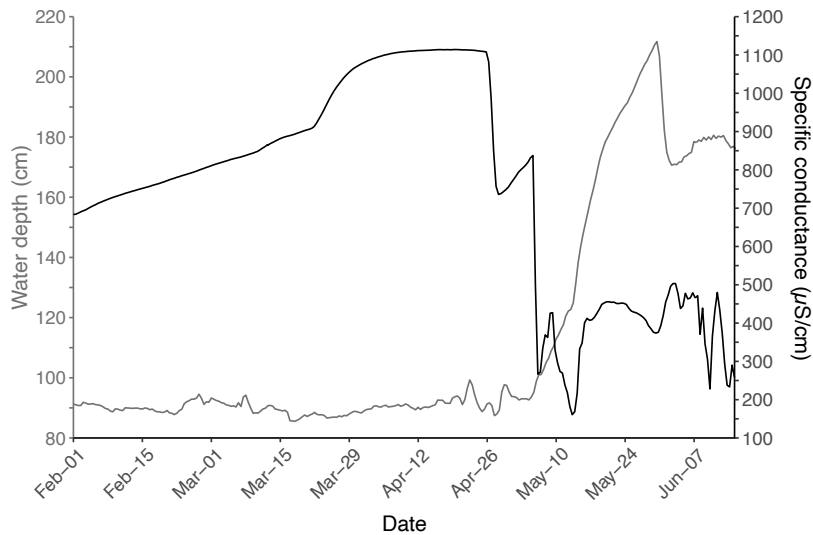


Figure 3. Measurements of water depth (gray line) and specific conductance (black line) at Highway 130 Lake in 2017.

312

313

314 **4.2 Sediment characteristics**

315 The 333-cm core from HL extends to at least the early Holocene and contains
 316 predominantly carbonate sediment underlain by silicate clays (Fig. 4). The upper 303 cm
 317 contains from 5–55% organics and 5–90% carbonate; the core above the basal 30 cm has a mean
 318 carbonate content of 65%. In the basal unit, the carbonate content drops below 5%, which was
 319 too low for isotopic analysis. The age-depth model (black line with 2-sigma gray uncertainty
 320 band, Fig. 4, Table 2) reveals average net sediment accumulation rates of 18 cm/kyr (thousand
 321 years) from 11.7–4.4 ka and 45.5 cm/kyr from 4.4 ka to present. High rates of net sedimentation

Deleted: in

Deleted: in

Deleted: 1

325 correspond with intervals of high carbonate flux into the lake, indicating that authigenic
 326 carbonate production may largely control sedimentation rates. The carbonate content and
 327 carbonate flux, representing the mass of carbonates deposited per unit area per year, increased
 328 simultaneously with the sedimentation rate at 4.4 ka (Fig. 4), but the percent carbonate content
 329 subsequently declined until 4.0 ka. The radiocarbon age at 119-cm depth (3.072 ± 0.03 ka) has
 330 an age similar to the date at 67-cm depth (3.031 ± 0.02 ka), which may indicate a reworked
 331 upper age (black dots in Fig. 4). However, high total sediment and carbonate accumulation rates
 332 are inferred even if the upper age was excluded from the age-depth model.

333
 334

335 Table 2. Calibrated radiocarbon ages used for the age-depth model.

Deleted: 1

Lake	Core	Depth (cm)	Material	Lab number	Age (^{14}C yr BP)	Uncertainty (1σ , ^{14}C yr BP)	Calibrated age ranges (1σ , cal yr BP)		
							Median	Maximum	Minimum
Highway 130 Lake	2A	18	Charcoal	UCIAMS-194167	850	30	748	783	726
		67	Charcoal	UCIAMS-194168	2,900	20	3,033	3,070	2,996
	2B	119-121	Charcoal	UCIAMS-194169	2,925	15	3,073	3,144	3,004
		154-156	Charcoal	UCIAMS-194170	3,660	35	3,986	4,081	3,921
		193-195	Charcoal	UCIAMS-194171	3,840	20	4,241	4,290	4,157
		204	Charcoal	UCIAMS-194172	3,965	20	4,438	4,508	4,412
		239	Charcoal	UCIAMS-194173	6,210	60	7,096	7,132	7,007
		302	Charcoal	UCIAMS-194174	9,580	25	10,927	11,074	10,781

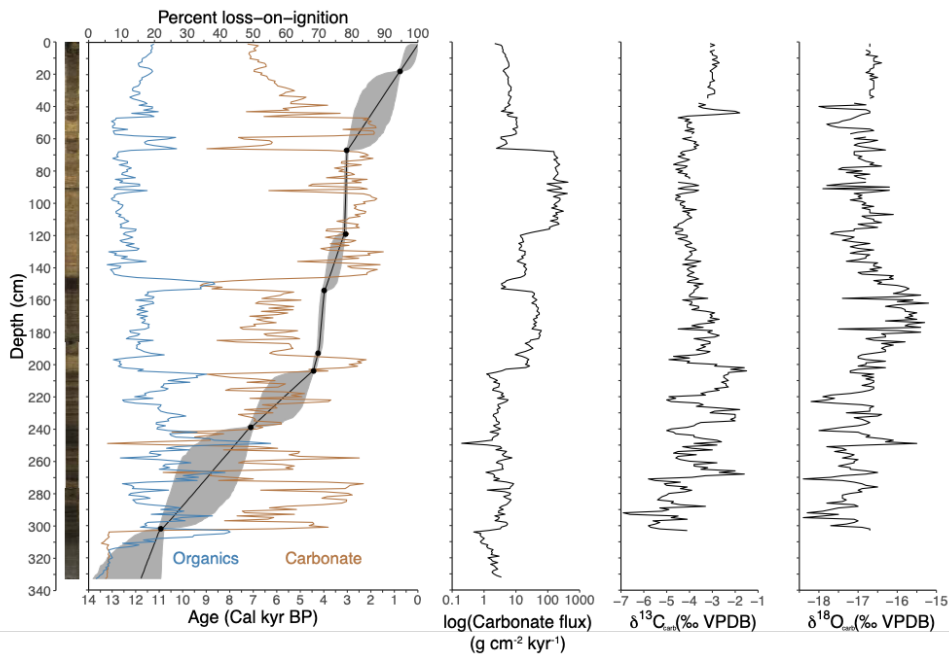


Figure 4. Percent organics, percent carbonate, carbonate flux, $\delta^{13}\text{C}_{\text{carb}}$, and $\delta^{18}\text{O}_{\text{carb}}$ are shown by depth alongside an image of the 333-cm-long sediment core from Highway 130 Lake. Radiocarbon ages (black dots) were used to create the age-depth model and gray uncertainty band (2 sigma).

338

339 4.3 Sedimentary oxygen and carbon isotopes

340 $\delta^{13}\text{C}_{\text{carb}}$ and $\delta^{18}\text{O}_{\text{carb}}$ in the upper 303 cm of sediment range from -6.9 to -1.5‰ and -18.4

341 to -15.2‰, respectively, and the mean isotope compositions become more positive over the

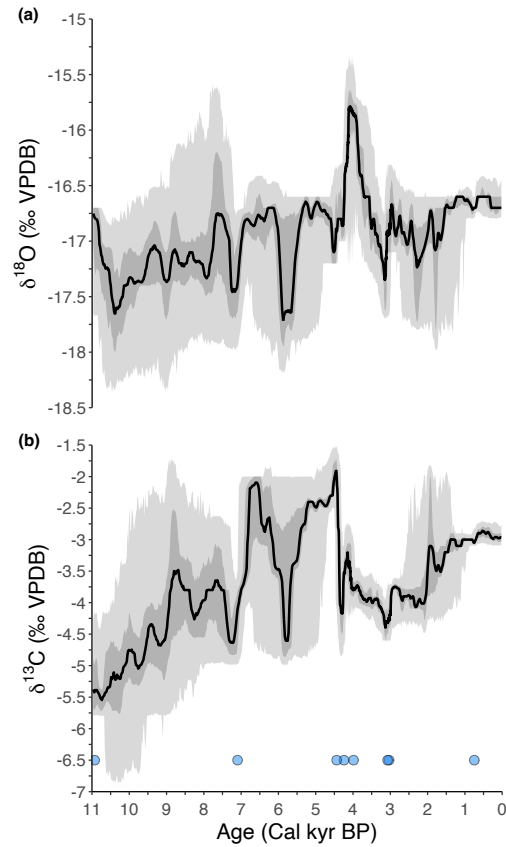
342 record, but there is no significant trend (Fig. 4). Variance in $\delta^{13}\text{C}_{\text{carb}}$ and $\delta^{18}\text{O}_{\text{carb}}$ is highest before

343 4.4 ka (below 200-cm depth) and lowest since 1.5 ka (above 40-cm depth; Fig. 5). Isotope

Deleted: long-term

Deleted: of $\delta^{18}\text{O}_{\text{carb}}$ is not statistically significant

346 excursions appear in both the slow and fast sedimentation intervals and when the carbonate flux
347 is both low and high (Fig. 4). $\delta^{18}\text{O}_{\text{carb}}$ peaks (2.9 standard deviations above the mean) from



348

Figure 5. $\delta^{18}\text{O}_{\text{carb}}$ (a) and $\delta^{13}\text{C}_{\text{carb}}$ (b) from Highway 130 Lake. The black line represents the median estimate of the ensemble regression, and the dark and light gray bands show the 50% and 95% highest-probability density regions, respectively. The blue dots indicate the calibrated radiocarbon ages used for the age-depth model (refer to Table 2 for calibrated age uncertainties).

Deleted: 1

349 approximately 4.2–4 ka, where four calibrated radiocarbon ages constrain the timing and indicate
350 a fast sedimentation rate (Fig. 5). The carbonate flux is high, but the carbonate content is low
351 (~55%) during this interval relative to the mean (Fig. 4).

352 Compared to the records for Bison and Yellow Lakes in Colorado (Anderson, 2011,
353 2012; Fig. 1), $\delta^{18}\text{O}_{\text{carb}}$ values of HL are several per mil lower with higher variance for most of
354 the Holocene (Fig. 6). This pattern changes in the late Holocene as carbonate in Bison Lake
355 becomes isotopically lighter than before and approaches the oxygen isotope composition of HL,
356 which maintains a relatively constant mean $\delta^{18}\text{O}_{\text{carb}}$ value. After approximately 1.5 ka, $\delta^{18}\text{O}_{\text{carb}}$
357 variability in HL drops to near the analytical uncertainty ($\pm 0.2\text{‰}$) while the other records show

358 increased variably (Fig. 6). ~~Despite an increase in summer lake-water $\delta^{18}\text{O}$ from -17.8 to -10.8‰~~
359 ~~today (thick black line, Fig. 2), $\delta^{18}\text{O}_{\text{carb}}$ values at HL since 1.5 ka only reached a maximum of -~~
360 ~~16.4‰ and the core-top value is -16.7‰ (Fig. 5). Based on measured lake-water $\delta^{18}\text{O}$ and mean~~
361 ~~water temperatures during the biweekly intervals in which samples were collected from June~~
362 ~~through October, core-top $\delta^{18}\text{O}_{\text{carb}}$ at HL should range from -17.4 – -10.3‰ based on a standard~~
363 ~~$\delta^{18}\text{O}$ -temperature model for estimating $\delta^{18}\text{O}_{\text{carb}}$ (Leng and Marshall, 2004); using the full range~~
364 ~~of lake-water temperatures measured through the annual cycle produces a range of -18.3 – -~~
365 ~~8.9‰.~~

Deleted: A positive excursion of similar magnitude also occurred from 7.8–7.3 ka, but aligns with high organic content and low $\delta^{13}\text{C}_{\text{carb}}$, carbonate content, carbonate flux, and total net sediment accumulation.

Moved (insertion) [2]

Deleted: , which is closer to the composition of groundwater (open squares, Fig. 2) than the mid- to late-summer lake-water- $\delta^{18}\text{O}$ values (black circles, Fig. 2)

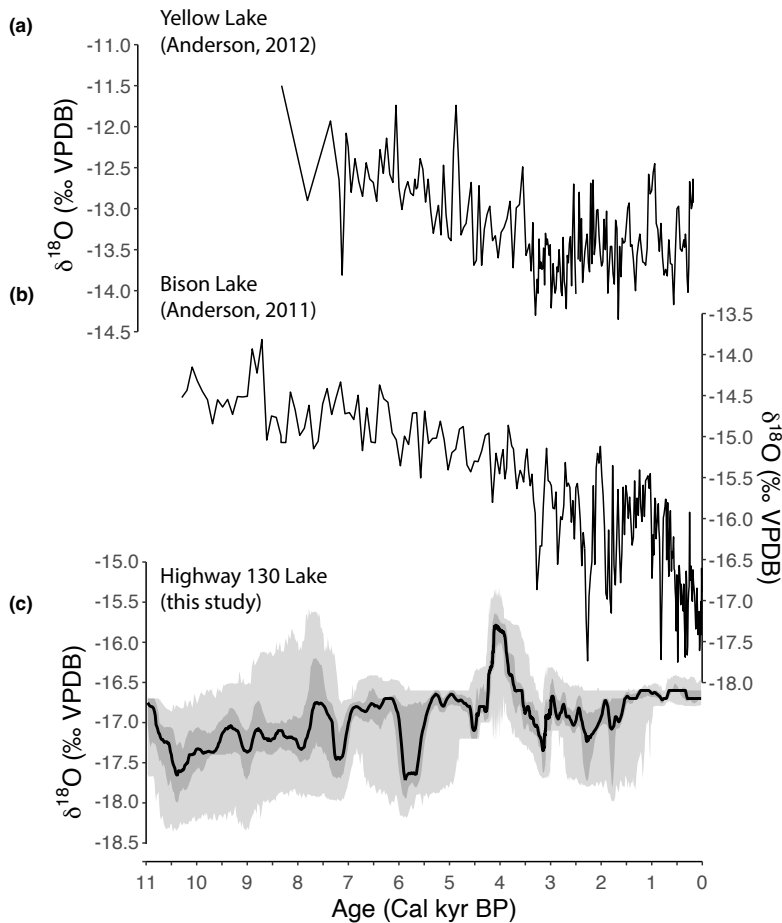


Figure 6. $\delta^{18}\text{O}_{\text{carb}}$ records from (a) Yellow Lake (Anderson, 2012), (b) Bison Lake (Anderson, 2011), and (c) Highway 130 Lake. In (c) the black line represents the median estimate of the ensemble regression, and the dark and light gray bands show the 50% and 95% highest-probability density regions, respectively.

Deleted: (black)

Deleted: ,

Deleted: Bison Lake (purple; Anderson, 2011), and Yellow Lake (yellow; Anderson, 2012) vary despite their similar locations and elevations.

381 5. **Discussion**

382 ***5.1 Evidence of the 4.2 ka drought in the southern Rocky Mountains***

383 Peak $\delta^{18}\text{O}_{\text{carb}}$ in HL indicates an abrupt decline in effective moisture or at least a decline
384 in the ratio of snowfall to rain in the Medicine Bow Mountains from approximately 4.2–4 ka
385 (Fig. 5) when evidence from additional climate records shows that aridity affected the southern
386 Rocky Mountains and portions of the Great Plains (Carter et al., 2013; Halfen & Johnson, 2013;
387 Stokes & Gaylord, 1993). The isotope composition of mean annual precipitation potentially
388 became heavier as snowfall declined relative to rain, causing HL's lake-water $\delta^{18}\text{O}$ and $\delta^{18}\text{O}_{\text{carb}}$
389 to increase. High evaporation could have also amplified these changes. The highest $\delta^{18}\text{O}_{\text{carb}}$
390 values at HL coincide with the pollen-inferred precipitation and temperature changes at 4.2 ka at
391 Long Lake, which records two centuries of severe drought (Long Lake, Fig. 1; Carter et al.,
392 2013). The excursion also aligns with the longstanding evidence of drought in the Great Plains
393 and southern Rocky Mountains (dune fields, Fig. 1), where a rapid loss of grain-trapping
394 vegetation likely triggered several centuries of increased aeolian transport documented across
395 multiple dune fields (Booth et al., 2005; Forman et al., 2001; Halfen et al., 2010; Stokes &
396 Gaylord, 1993).

397 Taken together, the records suggest that rapid drying at around 4.2 ka was an important
398 climatic event in the Medicine Bow Mountains even if the drought is not a prominent feature in
399 other paleoclimate studies from the mid-latitude Rocky Mountains (Anderson et al., 2008;
400 Brunelle et al., 2013; Feiler et al., 1997; Johnson et al., 2013; Mensing et al., 2012; Minckley et
401 al., 2012; Shuman et al., 2010; Thompson et al., 1993; Whitlock & Bartlein, 1993), including the
402 nearby $\delta^{18}\text{O}_{\text{carb}}$ records from Bison and Yellow Lakes (Anderson, 2011, 2012). The spatial
403 patterns of late-Holocene hydroclimate changes in North America may have been complex

404 compared to other regions, such as the European continent where late-Holocene climate
405 variability appears more coherently in climate records (e.g., Deininger et al., 2017). For example,
406 drought status can differ significantly east and west of the Continental Divide, which lies
407 between HL and Bison Lakes. Still, the inconsistent evidence complicates interpretations of the
408 4.2 ka anomaly here and elsewhere (Bradley & Bakke, 2019).

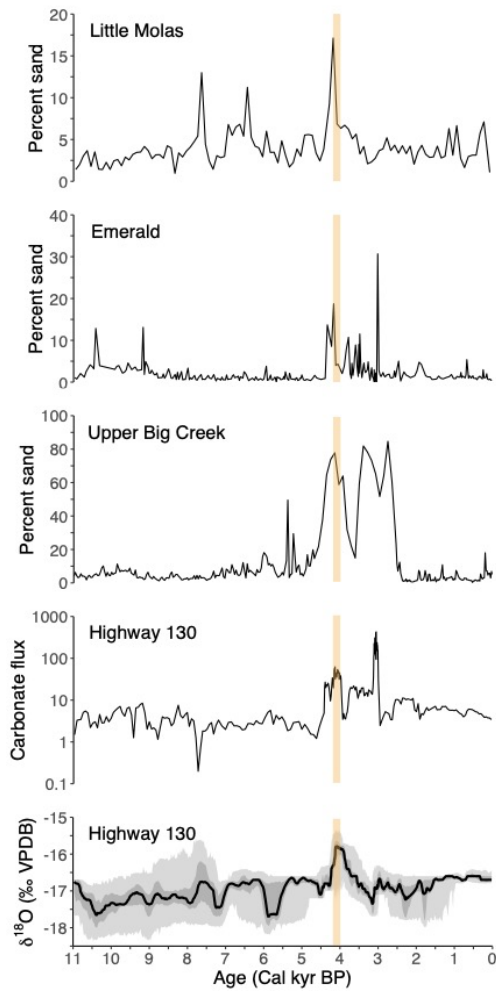
409 Some paleohydrologic evidence indicates, however, that the event may have been
410 extensive in the southern Rocky Mountains. Sedimentological changes in Little Molas, Emerald,
411 and Upper Big Creek lakes, all high-elevation lakes in Colorado (Fig. 1, Table 1), show
412 substantial hydrological transformation at around 4 ka matching the timing and scale of drought
413 inferred from HL's record (Fig. 7; Shuman et al., 2009a, 2014, 2015). The sediment
414 stratigraphies in these three lakes record low water levels that shifted shoreline sands to the
415 locations of cores collected in 1–5-m water depth today and thus indicate reduced effective
416 moisture at ca. 4.2–4 ka (orange shaded regions, Fig. 7). The median ages of sand layers,
417 indicative of low water at these sites, overlap and fall within the age distribution of the elevated
418 $\delta^{18}\text{O}_{\text{carb}}$ at HL and overlap with the ages of dune activity in southeast Wyoming (Halfen &
419 Johnson, 2013; Stokes & Gaylord, 1993); the high-elevation lake locations and geophysical site
420 surveys confirm that the shallow-water sands were not deposited by aeolian activity. Multiple
421 radiocarbon ages also constrain the interval of high carbonate accumulation to approximately
422 4.4–3 ka, but the sedimentation rate in the interval is sensitive

Deleted: 1 &

Deleted: 3.9

Deleted: gray

Deleted: A second prominent sand layer in Emerald and Upper Big Creek Lakes at ca. 3.1 ka (gray shaded regions, Fig. 7) indicates low effective moisture and overlaps with the maximum rate of carbonate accumulation at HL, but a second sand layer does not appear in Little Molas Lake and the $\delta^{18}\text{O}_{\text{carb}}$ values in HL are lower than at 4.2 ka. It took several centuries for $\delta^{18}\text{O}_{\text{carb}}$ values to rise and fall before and after the peak from 4.2–4 ka, but the excursion at 3.1 ka occurred within a century.



439

440

Figure 7. Spikes in the sand content of Little Molas, Emerald, and Upper Big Creek Lakes, located in high-elevation watersheds in Colorado (Fig. 1), align with the positive $\delta^{18}\text{O}_{\text{carb}}$ excursion at Highway 130 Lake and indicate low water from approximately 4.2–4 ka (orange shaded areas) resulting from low effective moisture (Shuman et al., 2009a, 2014, 2015).

Deleted: Another positive $\delta^{18}\text{O}_{\text{carb}}$ excursion at ca. 3.1 ka (gray shaded areas) aligns with intervals of low water at Emerald and Upper Big Creek Lakes.

441 to removal of one of the ages; if the age at ca. 3 ka is out of sequence, it may bias the peak rate of
442 sediment and carbonate accumulation toward high values (but not the timing of the $\delta^{18}\text{O}_{\text{carb}}$ peak,
443 Figures 4-7).

444 The rapid transition from deep-water muds to shallow-water sands as water levels
445 dropped in the Colorado lakes at around 4.2 ka corresponds with changes in pollen assemblages
446 in central Colorado (Jiménez-Moreno et al., 2019) and southeast Wyoming (Carter et al., 2013),
447 as well as with other evidence for drought in North America (Fig. 1, Table 1; Booth et al., 2004).
448 Similar sedimentological features found in lakes along the Atlantic margin from Maine to
449 Pennsylvania date to around 4.2 ka, for example, where the drought appears as one of multiple
450 events linked to circulation changes over the North Atlantic (Li et al., 2007; Marsicek et al.,
451 2013; Newby et al., 2014; Nolan, 2020; Shuman et al., 2019; Shuman & Burrell, 2017). The
452 sequences in the southern Rocky Mountains, however, include uniquely prominent
453 sedimentological changes from ca. 4.2–4 ka, which align with the single large positive $\delta^{18}\text{O}_{\text{carb}}$
454 excursion at HL.

455 Given the growing evidence of drought within the southern Rocky Mountains at ca. 4.2
456 ka, a lack of $\delta^{18}\text{O}_{\text{carb}}$ records of the event in the region, or in North America entirely, is surprising
457 (Anderson et al., 2016b; Konecky et al., 2020). However, individual sites respond to a varying
458 mixture of local and regional factors. The stratigraphic evidence of lake-level change in the
459 region is not entirely consistent either and may indicate interactions with different directions of
460 hydroclimate change across seasons, elevations, and latitudes. Stratigraphic features in Hidden
461 Lake, located in northern Colorado just south of Upper Big Creek Lake (Fig. 1) but several
462 hundred meters lower in elevation, document a rapid increase in effective moisture at around 4
463 ka (Shuman et al., 2009)—the opposite response of the surrounding lakes at higher elevations

Deleted: isotopic and

Deleted: 3.9

Deleted: associated with the widespread climatic anomaly

467 (Fig. 7). The wet phase was abrupt in onset and termination and lasted from around 4.4–3.7 ka,
468 based on multiple radiocarbon ages, and stands out amid an otherwise gradual trend towards
469 higher water levels since 6 ka (Shuman et al., 2009).

470 The low-elevation location of Hidden Lake may indicate an important role for increased
471 summer or fall rainfall when high-elevation lake levels declined in response to low winter
472 snowfall. Low winter snow can create favorable surface-energy conditions for strong summer
473 convective precipitation (Zhu et al. 2005). The combined effects could have favored the
474 unusually high $\delta^{18}\text{O}_{\text{carb}}$ at HL by positively shifting the isotope values of mean annual
475 precipitation and HL's water. Alternatively, the reversed hydrologic response of Hidden Lake
476 could indicate antiphased hydroclimate changes in the southern Rocky Mountains between high
477 and low elevations, which is consistent with modern responses to the El Niño-Southern
478 Oscillation (Preece et al., 2020). The active dune fields in east-central Wyoming, however, could
479 confound a simple interpretation of the elevational and seasonally antiphased hydrologic
480 changes, although their activity may depend on soil moisture derived from winter snow (Stokes
481 & Gaylord, 1993). Latitudinal hydroclimate variability could be an additional complicating
482 factor related to the dynamic boundary between the climates of the northern and southern Rocky
483 Mountains (Shinker, 2010; Wise, 2010). The comparison of the radiocarbon age uncertainties of
484 the 4.2 ka paleoshoreline sands at lake-level sites, including Emerald Lake in central Colorado
485 (Fig. 1 & 7), indicates a late-Holocene north-south moisture dipole extending across much of the
486 area described here (Shuman et al., 2014).

487 Given the potential prominence of the 4.2 ka drought at HL and other southern Rocky
488 Mountain records, it may have been uniquely severe in this region even if it had a complex
489 regional expression at broader spatial scales. The lake-level reconstructions from Colorado

Deleted: sites

Deleted: The combined effects could have favored the unusually high $\delta^{18}\text{O}_{\text{carb}}$ at HL.

493 contain evidence of other Holocene hydrologic changes (Fig. 7), but the records lack evidence
494 for multiple recurrent, multi-century hydroclimate changes recorded with the 4.2 ka event in
495 places like the Atlantic margin (Shuman et al., 2019). Elsewhere, aridity at 4.2 ka may represent
496 just one of several repeated drying events consistent with climate records and simulations from
497 around the world that show drought as a regular feature of late-Holocene climate variability (Arz
498 et al., 2006; Bradley & Bakke, 2019; Mayewski et al., 2004; Wanner et al., 2008; Wanner et al.,
499 2015; Yan & Liu, 2019). The mid-latitude Rocky Mountain records may suggest that the
500 midcontinent was insulated from some of the abrupt late-Holocene climate changes, possibly due
501 to its isolation from the ocean-atmosphere dynamics proposed to play key roles in Holocene
502 variability (Arz et al., 2006; Deininger et al., 2017; Jalali et al., 2019; Yan & Liu, 2019).

Deleted: and HL shows another positive excursion at 7.8 ka (Fig. 5)

503

504 **5.2 Varying $\delta^{18}O_{carb}$ trends in the southern Rocky Mountains**

505 The marked sensitivity of lake-water $\delta^{18}O$ to hydroclimate changes may make lacustrine
506 carbonates ideal indicators of past droughts like the 4.2 ka event, as documented by $\delta^{18}O_{carb}$
507 records outside of North America (e.g., Bini et al., 2019; Dean et al., 2015) and by our record at
508 HL (Fig. 5), but site-specific hydrologic conditions could complicate the signals. They may
509 generate inconsistent trends among records over both short (seasonal) and long (millennial)
510 timescales (Gibson et al., 2016; Shapley et al., 2008; Steinman & Abbott, 2013; Tyler et al.,
511 2007). Indeed, we observe such inconsistency in the southern Rocky Mountains (Fig. 6).

Deleted: Mark D.

512 The hydrologic controls, such as groundwater fluxes and basin morphology, can vary
513 based on a lake's geohydrological setting (Anderson et al., 2016; Dean et al., 2015). Modern
514 lake-water hydrogen and oxygen isotope measurements reveal stronger fractionation by
515 evaporation in HL (thick black line, Fig. 2) compared to Bison and Yellow Lakes (purple and

519 yellow lines, Fig. 2; Anderson, 2012), which exhibit a narrower range in modern water isotope
520 ~~compositions~~ and smaller deviation from the global meteoric water line. ~~The differences in~~
521 ~~hydrologic setting at each lake that produce this pattern are not assumed to override changes in~~
522 ~~lake-water $\delta^{18}\text{O}$ due to climate changes, such as drought.~~ However, the ~~isotopically light~~
523 carbonate at HL (Fig. 6) is antithetical to the expectation based on evaporatively enriched
524 summer waters (Fig. 2) ~~and suggests that the site may have been sensitive to seasonal dynamics~~
525 ~~not recorded by Bison or Yellow Lakes.~~ The pattern differs from the interpretation that the Bison
526 Lake $\delta^{18}\text{O}_{\text{carb}}$ was not strongly influenced by evaporation because it was isotopically lighter than
527 other sites like Yellow Lake (Anderson, 2011, 2012). ~~Given the modern water isotope values, we~~
528 had anticipated that $\delta^{18}\text{O}_{\text{carb}}$ from HL would be isotopically heavy compared to Bison and
529 Yellow Lakes, but track similar trends (Anderson, 2012). ~~However, HL lacks the prominent~~
530 ~~$\delta^{18}\text{O}_{\text{carb}}$ trend observed at these other sites (Fig. 6).~~

531 Differences in the timing of carbonate formation could explain the variability among the
532 records and their sensitivity to the 4.2 ka event. Because rain is isotopically heavier than snow,
533 decreasing snowpack in the watershed should positively shift the isotope composition of HL's
534 water and carbonates. A lower ratio of precipitation to evaporation could also cause a positive
535 shift if carbonates form in evaporated summer waters; however, if the precipitation of carbonates
536 occurs during winter or spring, then $\delta^{18}\text{O}_{\text{carb}}$ would track the relative contributions of snowfall
537 and rain to its water balance without modification by summer evaporation. Previous studies have
538 shown that the deposition of endogenic carbonate occurs predominantly in the warm summer
539 months when photosynthesis optimizes carbonate production by modifying dissolved CO_2
540 concentrations and pH (Leng & Marshall, 2004), but the isotopically light carbonate at HL may
541 contradict this expectation. The observed core-top $\delta^{18}\text{O}_{\text{carb}}$ value is lower than the calculated

Deleted: values

Deleted: (Anderson, 2012)

Deleted: is isotopically lighter than the other two

Deleted: , which

Moved down [3]: HL lacks the prominent $\delta^{18}\text{O}_{\text{carb}}$ trend observed at these other sites (Fig. 6).

Moved (insertion) [3]

548 fractionation of calcite formation in summer waters, which indicates that HL may not integrate
549 the range of summer lake-water $\delta^{18}\text{O}$ today as is assumed for Bison and Yellow Lakes (and
550 carbonate lakes in general).

551 We observe the same pattern in HL's sediment record. $\delta^{18}\text{O}_{\text{carb}}$ values were below the
552 mean at 6 ka (Fig. 5) when simulated estimates of evaporation rates in the Medicine Bow
553 Mountains were up to 30% higher than today (Morrill et al., 2019). The enhanced evaporation
554 may explain the more positive mid-Holocene $\delta^{18}\text{O}_{\text{carb}}$ at Bison and Yellow lakes relative to today
555 (Fig. 6), but if so, such enhanced summer evaporation did not affect $\delta^{18}\text{O}_{\text{carb}}$ at HL. Because the
556 early springtime deposition of carbonate could capture the isotopic signature of the lake water
557 early in the year, HL may be a better indicator of the snow-to-rain ratio represented by the
558 groundwater inflow into the lake than the seasonal isotopic enrichment of the lake waters by
559 evaporation later in the summer.

560 The year-round measurements of specific conductance show that conditions favorable for
561 carbonate precipitation may indeed be highest during late winter and spring. In 2017, specific
562 conductance of the water below the surface ice rose from 700 $\mu\text{S}/\text{cm}$ in early February to 1,115
563 $\mu\text{S}/\text{cm}$ by early April, and it remained above 1,000 $\mu\text{S}/\text{cm}$ throughout April (Fig. 3). These high
564 values would favor carbonate precipitation, whereas the summertime waters are more dilute.
565 Specific conductance of HL and other lakes within the watershed during the summer typically
566 does not exceed 300 $\mu\text{S}/\text{cm}$. Melting of lake ice and snowpack rapidly lowers the specific
567 conductance by early May and it remains between 250–300 $\mu\text{S}/\text{cm}$ for the remaining ice-free
568 months. The conductance likely remains lower than in winter despite evaporative enrichment of
569 the oxygen isotopes because of groundwater discharge into the lake (Rautio & Korkka-Niemi,
570 2011), which geophysical surveys, water temperatures, and stable summer water levels at HL

Deleted: Because the modern water isotope values poorly predicted $\delta^{18}\text{O}_{\text{carb}}$ trends, the different lakes may record past changes in different ways. HL may be a better indicator of winter snowpack than evaporation.

Deleted: We also find lower-than-expected $\delta^{18}\text{O}_{\text{carb}}$ values in the uppermost sediments.

Moved up [2]: Despite an increase in summer lake-water $\delta^{18}\text{O}$ from -17.8 to -10.8‰ today (thick black line, Fig. 2), $\delta^{18}\text{O}_{\text{carb}}$ values since 1.5 ka only reached a maximum of -16.4‰ and the core-top value is -16.7‰ (Fig. 5), which is closer to the composition of groundwater (open squares, Fig. 2) than the mid- to late-summer lake-water- $\delta^{18}\text{O}$ values (black circles, Fig. 2).

Deleted: Previous studies have shown that the deposition of endogenic carbonate occurs predominantly in the warm summer months when photosynthesis optimizes carbonate production by modifying dissolved CO_2 concentrations and pH (Leng & Marshall, 2004), but the isotopically light carbonate at HL may contradict this expectation. For comparison, the uppermost $\delta^{18}\text{O}_{\text{carb}}$ value of -14.9‰ in Bison Lake (purple line, Fig. 6) falls within the range in modern summer lake-water- $\delta^{18}\text{O}$ values of -16.7 to -13.5‰ (purple line, Fig. 2; Anderson, 2011). $\delta^{18}\text{O}_{\text{carb}}$ in HL, therefore, may not integrate the range of summer lake-water $\delta^{18}\text{O}$ as is assumed for Bison and Yellow Lakes (and carbonate lakes in general), but early springtime deposition of carbonate at HL could capture the signature of isotopically light lake water without modification by warm-season evaporation. →¶

599 support (Liefert et al., 2018). If so, ions exsolved from overlying ice raise the conductance of the
600 lake water and pore water within the bottom sediments beyond the concentration in groundwater
601 in winter (Adams & Lasenby, 1985), and create favorable conditions for the rapid deposition of
602 endogenic carbonate in early spring when the isotopic signal would not reflect evaporation or
603 isotopically heavy summer rainfall (open circles, Fig. 2). Spring carbonate formation could also
604 yield a different temperature-dependent effect on the $\delta^{18}\text{O}_{\text{carb}}$ in HL compared to the other lakes,
605 but the cold spring waters at HL should favor an increase, not decrease, in $\delta^{18}\text{O}_{\text{carb}}$. Indeed, all of
606 the readily expected process that could complicate a carbonate isotopic record should drive the
607 $\delta^{18}\text{O}_{\text{carb}}$ in the positive (not negative) direction and underscore the significance of the difference
608 between HL and the other lakes.

609 As an alternative explanation, the $\delta^{18}\text{O}_{\text{carb}}$ values could reflect changes in total
610 precipitation rather than seasonality effects because the inflow of Ca-bearing groundwater
611 (which should rise with precipitation) can increase carbonate production and lower $\delta^{18}\text{O}_{\text{carb}}$
612 values in alkaline lakes in both ice-free and ice-covered conditions (Shapley et al., 2005), but the
613 weak covariance of weight percent carbonate and $\delta^{18}\text{O}_{\text{carb}}$ suggest that rates of groundwater
614 inflow did not strongly influence $\delta^{18}\text{O}_{\text{carb}}$ (Fig. S1a). A weak covariance of $\delta^{13}\text{C}_{\text{carb}}$ and $\delta^{18}\text{O}_{\text{carb}}$
615 indicates short lake-water residence times throughout the lake's history (Fig. S1b; Drummond et
616 al., 1995; Talbot & Kelts, 1990), which could be consistent with rapid flowthrough that reduced
617 evaporative enrichment; removing values from 4.2-4 ka only marginally improves the
618 correlation.

619 A strong negative correlation of weight percent organics and carbonate ($R^2 = -0.79$)
620 suggests that carbonate abundance depends primarily on biological productivity that promoted
621 carbonate dissolution by releasing CO_2 and lowering pH (Fig S1c; Dean, 1999). Carbonate

622 content from 4.2–4 ka was below the mean despite low organic content (red dots, Fig. S1c) and a
623 high flux of carbonate (Fig. 4), which may represent a shift in HL’s water levels and chemistry
624 that favored both acidic conditions and isotopically heavy carbonate (red dots, Fig. S1). Down-
625 core shifts in $\delta^{18}\text{O}_{\text{carb}}$ produced by seasonal changes in the timing and rate of carbonate formation
626 have been proposed as potential sources of variability within individual records (Fronval et al.,
627 1995; Lamb et al., 2007; Steinman et al., 2012; Steinman & Abbott, 2013; Tyler et al., 2007) and
628 could play a role in the record at HL, but such differences could also generate the variability in
629 the long-term trends observed among records from the southern Rocky Mountains and elsewhere
630 (Bini et al., 2019; Konecky et al., 2020; Roberts et al., 2008).

631 Many non-climatic factors influence $\delta^{18}\text{O}_{\text{carb}}$, including carbonate phase and disequilibrium
632 effects, seasonality of precipitation, groundwater fluxes, the isotope compositions of precipitation
633 and groundwater, and local geology. However, such factors are unlikely sources of variability
634 among the regional $\delta^{18}\text{O}_{\text{carb}}$ records. Down-core carbonate phase changes are unlikely as only
635 calcite was present in the cores from HL, Bison Lake, and Yellow Lake. We also find no
636 evidence in the sediment core or modern setting at HL to indicate that anthropogenic influence or
637 biologically mediated precipitation of calcite substantially altered $\delta^{18}\text{O}_{\text{carb}}$ (e.g., carbonate
638 ostracod tests formed in disequilibrium with lake water). Disequilibrium effects associated with
639 biogenic carbonates generally increase $\delta^{18}\text{O}_{\text{carb}}$ (Holmes & Chivas, 2002; Leng & Marshall,
640 2004), which would be difficult to reconcile with the surprisingly negative mean and core-top
641 $\delta^{18}\text{O}_{\text{carb}}$ values at HL based on expectations from the strong enrichment of heavy isotopes by
642 evaporation today and predicted core-top $\delta^{18}\text{O}_{\text{carb}}$ values.

643 The seasonal balance of precipitation today is broadly similar among the sites (inset plot,
644 Fig. 2) and the calculated annual precipitation- $\delta^{18}\text{O}$ value is approximately 1‰ lower at HL than

Moved down [4]: Other factors that could affect $\delta^{18}\text{O}_{\text{carb}}$, such as precipitation patterns and biological disequilibrium effects, are unlikely sources of variability among the regional $\delta^{18}\text{O}_{\text{carb}}$ records.

Moved (insertion) [4]

Deleted: Other

Deleted: that could affect $\delta^{18}\text{O}_{\text{carb}}$, such as precipitation patterns and biological disequilibrium effects,

652 [at Bison and Yellow Lakes](http://waterisotopesDB.org) (<http://waterisotopesDB.org>). Annual temperature ranges are also
653 similar for the watersheds, making it unlikely that temperature dependence of fractionation could
654 explain the range in $\delta^{18}\text{O}_{\text{carb}}$ values recorded across the three records unless the different water
655 depths and groundwater influences altered the seasonal temperature progression among lakes.
656 The difference in temperature would need to be large ($\sim 12\text{ }^\circ\text{C}$) to explain the offset in $\delta^{18}\text{O}_{\text{carb}}$
657 between HL and Bison Lake (and larger for the offset between HL and Yellow Lake), which is
658 unrealistic given the sites' comparable locations and elevations and the relatively small
659 temperature changes at mid-latitudes since 11 ka (Marsicek et al., 2018). The range in $\delta^{18}\text{O}_{\text{carb}}$
660 calculated from the annual range in modern lake-water $\delta^{18}\text{O}$ at the lakes does match the observed
661 offsets in the $\delta^{18}\text{O}_{\text{carb}}$ records of HL, Bison, and Yellow Lakes. The timing of carbonate
662 formation thus remains a plausible mechanism for producing the differences. Installing sediment
663 traps during the ice-free season could test the timing of carbonate production.

664 ▼

665 6. Conclusions

666 $\delta^{18}\text{O}_{\text{carb}}$ from HL indicates an abrupt hydroclimate change in the southern Rocky
667 Mountains from approximately 4.2–4 ka that reduced effective moisture or caused less snow to
668 fall than today at high elevations in southern Wyoming. Other $\delta^{18}\text{O}_{\text{carb}}$ records from the region
669 do not document the drought (Fig. 6; Anderson, 2012), but the event's timing overlaps with
670 evidence of multi-century drought from pollen, lake stratigraphies, and dunes in the southern
671 Rocky Mountains (Carter et al., 2013; Halfen & Johnson, 2013; Shuman et al., 2009a, 2014,
672 2015; Stokes & Gaylord, 1993), the western Great Plains (Booth et al., 2005; Dean, 1997; Halfen
673 & Johnson, 2013; Mason et al., 1997; Stokes & Gaylord, 1993), and elsewhere around the world
674 (Nakamura et al., 2016; Di Rita & Magri, 2019; Scuderi et al., 2019; Xiao et al., 2018).

Deleted: We also find no evidence in the sediment core or modern lake setting to indicate that biologically mediated precipitation of calcite substantially altered $\delta^{18}\text{O}_{\text{carb}}$ at HL (e.g., by the accumulation of ostracod tests that precipitate carbonates in disequilibrium with lake water). Disequilibrium effects associated with biogenic carbonates generally increase $\delta^{18}\text{O}_{\text{carb}}$ (Holmes & Chivas, 2002; Leng & Marshall, 2004), which would be difficult to reconcile with the surprisingly negative mean and core-top $\delta^{18}\text{O}_{\text{carb}}$ values at HL. Down-core carbonate phase changes are also unlikely as we identified that only calcite was present using x-ray diffraction (XRD). ¶

687 The timing and magnitude of hydroclimate change in our record agrees with the
688 perspective of a widespread megadrought at around 4.2 ka (Weiss, 2016), but inconsistencies
689 among climate records suggests that (1) site-specific factors can prevent identification of the
690 patterns of abrupt hydroclimate changes, particularly in $\delta^{18}\text{O}_{\text{carb}}$ records; (2) the hydrologic
691 response in North America and likely elsewhere around the world was spatially complex; and (3)
692 the abrupt hydroclimate changes in the North American midcontinent were more pronounced
693 against background Holocene variability than in many regions such as the Atlantic margin.
694 Consequently, a prolonged ‘megadrought’ at 4.2 ka was likely a significant feature of the
695 hydroclimate history in the mid-latitude Rocky Mountains even if that is not true globally.

696

697 **Data availability**

698 Data related to this paper ~~are~~ available through the National Centers for Environmental
699 Information on the National Oceanic and Atmospheric Administration website:

700 ~~<https://www.ncdc.noaa.gov/paleo/study/34993>~~. The analyses were performed in R.

701

702 **Author contributions**

703 D. Liefert and B. Shuman contributed to the design and implementation of the research, to the
704 analysis of the results, and to the writing of the manuscript.

705

706 **Competing Interests**

707 ~~The authors declare that they have no conflict of interest.~~

708

709 **Acknowledgments**

Deleted: will be made

Deleted: <https://www.ncdc.noaa.gov/data-access/paleoclimatology-data>

713 This project was funded by the National Geographic Society (CP-064ER-17), U.S. National
714 Science Foundation P2C2 (EAR-1903729), the Wyoming Center for Environmental Hydrology
715 and Geophysics via support from the U.S. NSF EPSCoR program (EPS-1208909), and the
716 Department of Geology and Geophysics at the University of Wyoming. We thank Andrew
717 Parsekian and Kevin Befus for field assistance and Andrew Flaim for assisting in sample
718 preparation.

719

720 **References**

- 721 Adams, W. P., & Lasenby, D. C. (1985). The Roles of Snow, Lake Ice and Lake Water in the Distribution of Major
722 Ions in the Ice Cover of a Lake. *Annals of Glaciology*, 7(February 1979), 202–207.
723 <https://doi.org/10.3189/s0260305500006170>
- 724 Alley, R. B., Mayewski, P. A., Sowers, T., Stuiver, M., Taylor, K. C., & Clark, P. U. (1997). Holocene climatic
725 instability: A prominent, widespread event 8200 yr ago. *Geology*, 25(6), 483–486.
726 [https://doi.org/10.1130/0091-7613\(1997\)025<0483:HCIAPW>2.3.CO;2](https://doi.org/10.1130/0091-7613(1997)025<0483:HCIAPW>2.3.CO;2)
- 727 Anderson, L. (2011). Holocene record of precipitation seasonality from lake calcite $\delta^{18}O$ in the central Rocky
728 Mountains, United States. *Geology*, 39(3), 211–214. <https://doi.org/10.1130/G31575.1>
- 729 Anderson, L. (2012). Rocky Mountain hydroclimate: Holocene variability and the role of insolation, ENSO, and the
730 North American Monsoon. *Global and Planetary Change*, 92–93, 198–208.
731 <https://doi.org/10.1016/j.gloplacha.2012.05.012>
- 732 Anderson, L., Berkelhammer, M., Barron, J. A., Steinman, B. A., Finney, B. P., & Abbott, M. B. (2016a). Lake
733 oxygen isotopes as recorders of North American Rocky Mountain hydroclimate: Holocene patterns and
734 variability at multi-decadal to millennial time scales. *Global and Planetary Change*, 137, 131–148.
735 <https://doi.org/10.1016/j.gloplacha.2015.12.021>
- 736 Anderson, L., Berkelhammer, M., Barron, J. A., Steinman, B. A., Finney, B. P., & Abbott, M. B. (2016b). Lake
737 oxygen isotopes as recorders of North American Rocky Mountain hydroclimate: Holocene patterns and
738 variability at multi-decadal to millennial time scales. *Global and Planetary Change*, 137, 131–148.
739 <https://doi.org/10.1016/j.gloplacha.2015.12.021>

740 Anderson, R. S., Allen, C. D., Toney, J. L., Jass, R. B., & Bair, A. N. (2008). Holocene vegetation and fire regimes
741 in subalpine and mixed conifer forests, southern Rocky Mountains, USA. *International Journal of Wildland*
742 *Fire*, 17(1), 96. <https://doi.org/10.1071/WF07028>

743 Arz, H. W., Lamy, F., & Pätzold, J. (2006). A pronounced dry event recorded around 4.2 ka in brine sediments from
744 the northern Red Sea. *Quaternary Research*, 66(3), 432–441. <https://doi.org/10.1016/j.yqres.2006.05.006>

745 Ault, T. R., George, S. S., Smerdon, J. E., Coats, S., Mankin, J. S., Carrillo, C. M., et al. (2018). A robust null
746 hypothesis for the potential causes of megadrought in Western North America. *Journal of Climate*, 31(1), 3–
747 24. <https://doi.org/10.1175/JCLI-D-17-0154.1>

748 Bello, R., & Smith, J. D. (1990). The Effect of Weather Variability on the Energy Balance of a Lake in the Hudson
749 Bay Lowlands , Canada. *INSTAAR, University of Colorado*, 22(1), 98–107.

750 Bini, M., Zanchetta, G., Perçoiu, A., Cartier, R., Català, A., Cacho, I., et al. (2019). The 4.2 ka BP Event in the
751 Mediterranean region: An overview. *Climate of the Past*, 15(2), 555–577. [https://doi.org/10.5194/cp-15-555-](https://doi.org/10.5194/cp-15-555-2019)
752 2019

753 Booth, R. K., Jackson, S. T., Forman, S. L., Kutzbach, J. E., Bettis, E. A., Kreig, J., & Wright, D. K. (2005). A
754 severe centennial-scale drought in mid-continental North America 4200 years ago and apparent global
755 linkages. *Holocene*, 15(3), 321–328. <https://doi.org/10.1191/0959683605hl825ft>

756 Bradley, R. S., & Bakke, J. (2019). Is there evidence for a 4.2 ka BP event in the northern North Atlantic region?
757 *Climate of the Past*, 15(5), 1665–1676. <https://doi.org/10.5194/cp-15-1665-2019>

758 Brunelle, A., Minckley, T. A., Lips, E., & Burnett, P. (2013). A record of Lateglacial/Holocene environmental
759 change from a high-elevation site in the Intermountain West, USA. *Journal of Quaternary Science*, 28(1),
760 103–112. <https://doi.org/10.1002/jqs.2600>

761 Carter, V. A., Brunelle, A., Minckley, T. A., Dennison, P. E., & Power, M. J. (2013). Regionalization of fire regimes
762 in the Central Rocky Mountains, USA. *Quaternary Research (United States)*, 80(3), 406–416.
763 <https://doi.org/10.1016/j.yqres.2013.07.009>

764 Carter, V. A., Shinker, J. J., & Preece, J. (2018). Drought and vegetation change in the central Rocky Mountains and
765 western Great Plains: Potential climatic mechanisms associated with megadrought conditions at 4200 cal yr
766 BP. *Climate of the Past*, 14(8), 1195–1212. <https://doi.org/10.5194/cp-14-1195-2018>

767 Clark, P. U., Webb, R. S., & Keigwin, L. D. (1999). *Mechanisms of global climate change at millennial time scales.*

768 Washington, DC: American Geophysical Union.

769 Dean, J. R., Jones, M. D., Leng, M. J., Noble, S. R., Metcalfe, S. E., Sloane, H. J., et al. (2015). Eastern
770 Mediterranean hydroclimate over the late glacial and Holocene, reconstructed from the sediments of Nar lake,
771 central Turkey, using stable isotopes and carbonate mineralogy. *Quaternary Science Reviews*, *124*, 162–174.
772 <https://doi.org/10.1016/j.quascirev.2015.07.023>

773 Dean, W. E. (1997). Rates, timing, and cyclicity of Holocene eolian activity in north-central United States: Evidence
774 from varved lake sediments. *Geology*, *25*(4), 331–334. [https://doi.org/10.1130/0091-](https://doi.org/10.1130/0091-7613(1997)025<0331:RTACOH>2.3.CO;2)
775 [7613\(1997\)025<0331:RTACOH>2.3.CO;2](https://doi.org/10.1130/0091-7613(1997)025<0331:RTACOH>2.3.CO;2)

776 Dean, W. E. (1999). The carbon cycle and biogeochemical dynamics in lake sediments. *Journal of Paleolimnology*,
777 *21*(4), 375–393. <https://doi.org/10.1023/A:1008066118210>

778 Deininger, M., McDermott, F., Mudelsee, M., Werner, M., Frank, N., & Mangini, A. (2017). Coherency of late
779 Holocene European speleothem $\delta^{18}\text{O}$ records linked to North Atlantic Ocean circulation. *Climate Dynamics*,
780 *49*(1–2), 595–618. <https://doi.org/10.1007/s00382-016-3360-8>

781 Denniston, R. F., Gonzalez, L. A., Baker, R. G., Asmerom, Y., Reagan, M. K., Edwards, R. L., & Alexander, E. C.
782 (1992). Speleothem evidence for Holocene fluctuations of the prairie-forest ecotone. *Geology*, *20*, 671–676.

783 Drummond, C. N., Patterson, W. P., & Walker, J. C. G. (1995). Climatic forcing of carbon-oxygen isotopic
784 covariance in temperate-region marl lakes. *Geology*, *23*(11), 1031. [https://doi.org/10.1130/0091-](https://doi.org/10.1130/0091-7613(1995)023<1031:cfocoi>2.3.co;2)
785 [7613\(1995\)023<1031:cfocoi>2.3.co;2](https://doi.org/10.1130/0091-7613(1995)023<1031:cfocoi>2.3.co;2)

786 Feiler, E. J., Scott, R., & Koehler, A. (2017). Late Quaternary Paleoenvironments of the White River Plateau ,
787 Colorado , U . S . A . Author (s): Eric J . Feiler , R . Scott Anderson and Peter A . Koehler Published by :
788 INSTAAR , University of Colorado Stable URL : <http://www.jstor.org/stable/1551836>, *29*(1), 53–62.

789 Forman, S. L., Oglesby, R., & Webb, R. S. (2001). Temporal and spatial patterns of Holocene dune activity on the
790 Great Plains of North America: Megadroughts and climate links. *Global and Planetary Change*, *29*(1–2), 1–
791 29. [https://doi.org/10.1016/S0921-8181\(00\)00092-8](https://doi.org/10.1016/S0921-8181(00)00092-8)

792 Fronval, T., Jensen, N. B., & Buchardt, B. (1995). Oxygen isotope disequilibrium precipitation of calcite in Lake
793 Arreso, Denmark. *Geology*, *23*(5), 463–466. [https://doi.org/10.1130/0091-](https://doi.org/10.1130/0091-7613(1995)023<0463:OIDPOC>2.3.CO;2)
794 [7613\(1995\)023<0463:OIDPOC>2.3.CO;2](https://doi.org/10.1130/0091-7613(1995)023<0463:OIDPOC>2.3.CO;2)

795 Gibson, J. J., Birks, S. J., Yi, Y., Moncur, M. C., & McEachern, P. M. (2016). Stable isotope mass balance of fifty

796 lakes in central Alberta: Assessing the role of water balance parameters in determining trophic status and lake
797 level. *Journal of Hydrology: Regional Studies*, 6, 13–25. <https://doi.org/10.1016/j.ejrh.2016.01.034>

798 Von Grafenstein, U., Erlenkeuser, H., Müller, J., Jouzel, J., & Johnsen, S. (1998). The cold event 8200 years ago
799 documented in oxygen isotope records of precipitation in Europe and Greenland. *Climate Dynamics*, 14(2),
800 73–81. <https://doi.org/10.1007/s003820050210>

801 Halfen, A. F., & Johnson, W. C. (2013). A review of Great Plains dune field chronologies. *Aeolian Research*, 10,
802 135–160. <https://doi.org/10.1016/j.aeolia.2013.03.001>

803 Halfen, A. F., Fredlund, G. G., & Mahan, S. A. (2010). Holocene stratigraphy and chronology of the Casper Dune
804 Field, Casper, Wyoming, USA. *Holocene*, 20(5), 773–783. <https://doi.org/10.1177/0959683610362812>

805 Henderson, A. K., & Shuman, B. N. (2009). Hydrogen and oxygen isotopic compositions of lake water in the
806 western United States. *Geological Society of America Bulletin*, 121(7–8), 1179–1189.
807 <https://doi.org/10.1130/B26441.1>

808 Holmes, J. A., & Chivas, A. R. (2002). Ostracod shell chemistry—overview. *Geophysical Union Geophysical*
809 *Monograph Series*, 131, 185–204.

810 Houston, R. S., & Karlstrom, K. E. (1992). Geologic map of Precambrian metasedimentary rocks of the Medicine
811 Bow Mountains, Albany and Carbon counties, Wyoming. *U.S. Geological Survey Miscellaneous*
812 *Investigations Map, I-2280. Sc.*

813 Huang, C. C., Pang, J., Zha, X., Su, H., & Jia, Y. (2011). Extraordinary floods related to the climatic event at 4200 a
814 BP on the Qishuihe River, middle reaches of the Yellow River, China. *Quaternary Science Reviews*, 30(3–4),
815 460–468. <https://doi.org/10.1016/j.quascirev.2010.12.007>

816 Jalali, B., Sicre, M. A., Azuara, J., Pellichero, V., & Combourieu-Nebout, N. (2019). Influence of the North Atlantic
817 subpolar gyre circulation on the 4.2 ka BP event. *Climate of the Past*, 15(2), 701–711.
818 <https://doi.org/10.5194/cp-15-701-2019>

819 Jiménez-Moreno, G., Anderson, R. S., Shuman, B. N., & Yackulic, E. (2019). Forest and lake dynamics in response
820 to temperature, North American monsoon and ENSO variability during the Holocene in Colorado (USA).
821 *Quaternary Science Reviews*, 211, 59–72. <https://doi.org/10.1016/j.quascirev.2019.03.013>

822 Johnson, B. G., Jiménez-Moreno, G., Eppes, M. C., Diemer, J. A., & Stone, J. R. (2013). A multiproxy record of
823 postglacial climate variability from a shallowing, 12-m deep sub-alpine bog in the southeastern San Juan

824 Mountains of Colorado, USA. *The Holocene*, 23(7), 1028–1038. <https://doi.org/10.1177/0959683613479682>

825 Kahle, D., & Wickham, H. (2013). ggmap: Spatial Visualization with ggplot2. *The R Journal*, 5(1), 144–161.

826 Konecky, B. L., McKay, N. P., Sidorova, O. V. C., Comas-bru, L., Dassié, P., Delong, K. L., et al. (2020). The Iso2k
827 Database: A global compilation of paleo- $\delta^{18}\text{O}$ and $\delta^2\text{H}$ records to aid understanding of Common Era climate.
828 *Earth Syst. Sci. Data Discuss.*, (In review). Retrieved from <https://doi.org/10.5194/essd-2020-5>

829 Lamb, H. F., Leng, M. J., Telford, R. J., Ayenew, T., & Umer, M. (2007). Oxygen and carbon isotope composition
830 of authigenic carbonate from an Ethiopian lake: A climate record of the last 2000 years. *Holocene*, 17(4), 517–
831 526. <https://doi.org/10.1177/0959683607076452>

832 Leng, M. J., & Marshall, J. D. (2004). Palaeoclimate interpretation of stable isotope data from lake sediment
833 archives. *Quaternary Science Reviews*, 23(7–8), 811–831. <https://doi.org/10.1016/j.quascirev.2003.06.012>

834 Li, Y. X., Yu, Z., & Kodama, K. P. (2007). Sensitive moisture response to Holocene millennial-scale climate
835 variations in the Mid-Atlantic region, USA. *Holocene*, 17(1), 3–8. <https://doi.org/10.1177/0959683606069386>

836 Liefert, D. T., Shuman, B. N., Parsekian, A. D., & Mercer, J. J. (2018). Why Are Some Rocky Mountain Lakes
837 Ephemeral? *Water Resources Research*, 54(8), 5245–5263. <https://doi.org/10.1029/2017WR022261>

838 Marsicek, J., Shuman, B. N., Bartlein, P. J., Shafer, S. L., & Brewer, S. (2018). Reconciling divergent trends and
839 millennial variations in Holocene temperatures. *Nature*, 554(7690), 92–96.
840 <https://doi.org/10.1038/nature25464>

841 Marsicek, J. P., Shuman, B., Brewer, S., Foster, D. R., & Oswald, W. W. (2013). Moisture and temperature changes
842 associated with the mid-Holocene Tsuga decline in the northeastern United States. *Quaternary Science
843 Reviews*, 80, 129–142. <https://doi.org/10.1016/j.quascirev.2013.09.001>

844 Mason, J. P., Swinehart, J. B., & Loope, D. B. (1997). Holocene history of lacustrine and marsh sediments in a
845 dune-blocked drainage, Southwestern Nebraska Sand Hills, U.S.A. *Journal of Paleolimnology*, 17(1), 67–83.
846 <https://doi.org/10.1023/A:1007917110965>

847 Mayewski, P. A., Rohling, E. E., Stager, J. C., Karlén, W., Maasch, K. A., Meeker, L. D., et al. (2004). Holocene
848 climate variability. *Quaternary Research*, 62(3), 243–255. <https://doi.org/10.1016/j.yqres.2004.07.001>

849 [McKay, N. P., Emile-Geay, J., and Khider, D.: geoChronR – an R package to model, analyze,
850 and visualize age-uncertain data. *Geochronology*, 3, 149–169, <https://doi.org/10.5194/gchron-3-149-2021>,
851 \[2021\]\(#\).](#)

Field Code Changed

852 Mensing, S., Korfmacher, J., Minckley, T., & Musselman, R. (2012). A 15,000 year record of vegetation and
853 climate change from a treeline lake in the Rocky Mountains, Wyoming, USA. *The Holocene*, 22(7), 739–748.
854 <https://doi.org/10.1177/0959683611430339>

855 Minckley, T. A., Shriver, R. K., & Shuman, B. (2012). Resilience and regime change in a southern Rocky Mountain
856 ecosystem during the past 17000 years TL - 82. *Ecological Monographs*, 82 VN-r(1), 49–68.
857 <https://doi.org/10.1890/11-0283.1>

858 Mock, C. . (1996). Climate controls and spatial variations of precipitation in the western United States. *Journal of*
859 *Climate*, 9, 1111–1125.

860 Morrill, C., Meador, E., Livneh, B., Liefert, D. T., & Shuman, B. N. (2019). Quantitative model-data comparison of
861 mid-Holocene lake-level change in the central Rocky Mountains. *Climate Dynamics*, 0(0), 0.
862 <https://doi.org/10.1007/s00382-019-04633-3>

863 Musselman, R. C., Connell, B. H., Conrad, M. A., Dufford, R. G., Fox, D. G., Haines, J. D., et al. (1992). The
864 Glacier Lakes Ecosystem Experiments Site.

865 Nakamura, A., Yokoyama, Y., Maemoku, H., Yagi, H., Okamura, M., Matsuoka, H., et al. (2016). Weak monsoon
866 event at 4.2 ka recorded in sediment from Lake Rara, Himalayas. *Quaternary International*, 397, 349–359.
867 <https://doi.org/10.1016/j.quaint.2015.05.053>

868 Newby, P. E., Shuman, B. N., Donnelly, J. P., Karnauskas, K. B., & Marsicek, J. (2014). Centennial-to-millennial
869 hydrologic trends and variability along the North Atlantic Coast, USA, during the Holocene. *Geophysical*
870 *Research Letters*, 41(12), 4300–4307. <https://doi.org/10.1002/2014GL060183>

871 Nolan, C. (2020). *Using Co-Located Lake and Bog Records to Improve Inferences on Late Quaternary Climate and*
872 *Ecology*.

873 Parnell, A. C., Haslett, J., Allen, J. R. M., Buck, C. E., & Huntley, B. (2008). A flexible approach to assessing
874 synchronicity of past events using Bayesian reconstructions of sedimentation history. *Quaternary Science*
875 *Reviews*, 27(19–20), 1872–1885. <https://doi.org/10.1016/j.quascirev.2008.07.009>

876 Preece, J. R., Shinker, J. J., Riebe, C. S., & Minckley, T. A. (2020). Elevation-dependent precipitation response to El
877 Niño-Southern oscillation revealed in headwater basins of the US central Rocky Mountains. *International*
878 *Journal of Climatology*, (November 2019), 1–12. <https://doi.org/10.1002/joc.6790>

879 Railsback, L. B., Liang, F., Brook, G. A., Voarintsoa, N. R. G., Sletten, H. R., Marais, E., et al. (2018). The timing,

880 two-pulsed nature, and variable climatic expression of the 4.2 ka event: A review and new high-resolution
881 stalagmite data from Namibia. *Quaternary Science Reviews*, 186, 78–90.
882 <https://doi.org/10.1016/j.quascirev.2018.02.015>

883 Ran, M., & Chen, L. (2019). The 4.2 ka BP climatic event and its cultural responses. *Quaternary International*,
884 (April), 0–1. <https://doi.org/10.1016/j.quaint.2019.05.030>

885 Rautio, A., & Korkka-Niemi, K. (2011). Characterization of groundwater-lake water interactions at Pyhäjärvi, a lake
886 in SW Finland. *Boreal Environment Research*, 16(5), 363–380.

887 Renssen, H., Goosse, H., & Muscheler, R. (2006). Coupled climate model simulation of Holocene cooling events:
888 oceanic feedback amplifies solar forcing, 79–90.

889 Di Rita, F., & Magri, D. (2019). The 4.2 ka event in the vegetation record of the central Mediterranean. *Climate of*
890 *the Past*, 15(1), 237–251. <https://doi.org/10.5194/cp-15-237-2019>

891 Roberts, N., Jones, M. D., Benkaddour, A., Eastwood, W. J., Filippi, M. L., Frogley, M. R., et al. (2008). Stable
892 isotope records of Late Quaternary climate and hydrology from Mediterranean lakes: the ISOMED synthesis.
893 *Quaternary Science Reviews*. <https://doi.org/10.1016/j.quascirev.2008.09.005>

894 Roland, T. P., Caseldine, C. J., Charman, D. J., Turney, C. S. M., & Amesbury, M. J. (2014). Was there a “4.2ka
895 event” in Great Britain and Ireland? Evidence from the peatland record. *Quaternary Science Reviews*, 83, 11–
896 27. <https://doi.org/10.1016/j.quascirev.2013.10.024>

897 Rosenberry, D. O., & LaBaugh, J. W. (2008). *Field Techniques for Estimating Water Fluxes Between Surface Water*
898 *and Ground Water*. <https://doi.org/10.3133/tm4D2>

899 Scuderi, L. A., Yang, X., Ascoli, S. E., & Li, H. (2019). The 4.2 ka BP Event in northeastern China: A geospatial
900 perspective. *Climate of the Past*, 15(1), 367–375. <https://doi.org/10.5194/cp-15-367-2019>

901 Shapley, M. D., Ito, E., & Donovan, J. J. (2005). Authigenic calcium carbonate flux in groundwater-controlled
902 lakes: Implications for lacustrine paleoclimate records. *Geochimica et Cosmochimica Acta*, 69(10), 2517–
903 2533. <https://doi.org/10.1016/j.gca.2004.12.001>

904 Shapley, Mark D., Ito, E., & Donovan, J. J. (2008). Isotopic evolution and climate paleorecords: Modeling boundary
905 effects in groundwater-dominated lakes. *Journal of Paleolimnology*, 39(1), 17–33.
906 <https://doi.org/10.1007/s10933-007-9092-3>

907 Shinker, J. J. (2010). Visualizing spatial heterogeneity of western U.S. climate variability. *Earth Interactions*,

908 14(10). <https://doi.org/10.1175/2010EI323.1>

909 Shuman, B., Henderson, A. K., Colman, S. M., Stone, J. R., Fritz, S. C., Stevens, L. R., et al. (2009). Holocene lake-
910 level trends in the Rocky Mountains, U.S.A. *Quaternary Science Reviews*, 28(19–20), 1861–1879.
911 <https://doi.org/10.1016/j.quascirev.2009.03.003>

912 Shuman, B., Pribyl, P., Minckley, T. A., & Shinker, J. J. (2010). Rapid hydrologic shifts and prolonged droughts in
913 Rocky Mountain headwaters during the Holocene. *Geophysical Research Letters*.
914 <https://doi.org/10.1029/2009GL042196>

915 Shuman, B. N., & Burrell, S. A. (2017). Centennial to millennial hydroclimatic fluctuations in the humid northeast
916 United States during the Holocene. *Quaternary Research (United States)*, 88(3), 514–524.
917 <https://doi.org/10.1017/qua.2017.62>

918 Shuman, B. N., Carter, G. E., Hougardy, D. D., Powers, K., & Shinker, J. J. (2014). A north-south moisture dipole at
919 multi-century scales in the Central and Southern Rocky Mountains, U.S.A., during the late Holocene. *Rocky*
920 *Mountain Geology*, 49(1), 33–49. <https://doi.org/10.2113/gsrocky.49.1.33>

921 Shuman, B. N., Pribyl, P., & Buettner, J. (2015). Hydrologic changes in Colorado during the mid-Holocene and
922 Younger Dryas. *Quaternary Research (United States)*, 84(2), 187–199.
923 <https://doi.org/10.1016/j.yqres.2015.07.004>

924 Shuman, B. N., Marsicek, J., Oswald, W. W., & Foster, D. R. (2019). Predictable hydrological and ecological
925 responses to Holocene North Atlantic variability. *Proceedings of the National Academy of Sciences of the*
926 *United States of America*, 116(13), 5985–5990. <https://doi.org/10.1073/pnas.1814307116>

927 Steinman, B. A., & Abbott, M. B. (2013). Isotopic and hydrologic responses of small, closed lakes to climate
928 variability: Hydroclimate reconstructions from lake sediment oxygen isotope records and mass balance
929 models. *Geochimica et Cosmochimica Acta*. <https://doi.org/10.1016/j.gca.2012.11.027>

930 Steinman, B. A., Abbott, M. B., Nelson, D. B., Stansell, N. D., Finney, B. P., Bain, D. J., & Rosenmeier, M. F.
931 (2012). Isotopic and hydrologic responses of small, closed lakes to climate variability: Comparison of
932 measured and modeled lake level and sediment core oxygen isotope records. *Geochimica et Cosmochimica*
933 *Acta*, 105, 455–471. <https://doi.org/10.1016/j.gca.2012.11.026>

934 Stewart, R. B., & Rouse, W. R. (1976). A Simple Method for Determining the Evaporation From Shallow Lakes and
935 Ponds. *Water Resources Research*, 12(4), 623–628. <https://doi.org/10.1029/WR012i004p00623>

- 936 Stokes, S., & Gaylord, D. R. (1993). Optical Dating of Holocene Dune Sands in the Ferris Dune Field, Wyoming.
937 *Quaternary Research*, 39, 274–281.
- 938 Talbot, M. R. (1990). A review of the palaeohydrological interpretation of carbon and oxygen isotopic ratios in
939 primary lacustrine carbonates. *Chemical Geology (Isotope Geosci. Sect.)*, 80, 261–279.
- 940 Talbot, M. R., & Kelts, K. (1990). Paleolimnological signatures from carbon and oxygen isotopic ratios in
941 carbonates from organic-rich lacustrine sediments. *Lacustrine Exploration: Case Studies and Modern*
942 *Analogs*, 99–112.
- 943 [Tan, L. C., An, Z. S., Cai, Y. J., & Long, H. \(2008\). Hydrological representation of the 4.2 ka BP event in](#)
944 [China and its global linkages. *Geological Review*, 54\(1\), 94-104.](#)
- 945 Thompson, R. S., Whitlock, C., Bartlein, P. J., Harrison, S. P., Geoffrey Spaulding, W. (1993). Climatic Changes in
946 the Western United States since 18,000 yr B.P. In P. J. Wright, Jr., H. E., Kutzbach, J. E., Webb III, T.,
947 Ruddiman, W. F., Street-Perrott, F. A., Bartlein (Ed.), *Global Climates since the Last Glacial Maximum* (pp.
948 468–513). University of Minnesota Press.
- 949 Tyler, J. J., Leng, M. J., & Arrowsmith, C. (2007). Seasonality and the isotope hydrology of Lochnagar, a Scottish
950 mountain lake: Implications for palaeoclimate research. *Holocene*, 17(6), 717–727.
951 <https://doi.org/10.1177/0959683607080513>
- 952 Walker, M., Gibbard, P., Head, M. J., Berkelhammer, M., Björck, S., Cheng, H., et al. (2019). Formal Subdivision
953 of the Holocene Series/Epoch: A Summary. *Journal of the Geological Society of India*, 93(2), 135–141.
954 <https://doi.org/10.1007/s12594-019-1141-9>
- 955 [Wang, Y., Cheng, H., Edwards, R. L., He, Y., Kong, X., An, Z., ... & Li, X. \(2005\). The Holocene Asian monsoon:](#)
956 [links to solar changes and North Atlantic climate. *Science*, 308\(5723\), 854-857.](#)
- 957 Wanner, H., Wanner, H., Mercolli, L., Mercolli, L., Grosjean, M., Grosjean, M., & Ritz, S. P. (2015). Holocene
958 climate variability and change: a data-based review. *Journal of the Geological Society*, 172(2), 254–263.
959 <https://doi.org/10.1144/jgs2013-101>
- 960 Wanner, Heinz, Beer, J., Bütikofer, J., Crowley, T. J., Cubasch, U., Flückiger, J., et al. (2008). Mid- to Late
961 Holocene climate change: an overview. *Quaternary Science Reviews*, 27(19–20), 1791–1828.
962 <https://doi.org/10.1016/j.quascirev.2008.06.013>
- 963 Wanner, Heinz, Solomina, O., Grosjean, M., Ritz, S. P., & Jetel, M. (2011). Structure and origin of Holocene cold

964 events. *Quaternary Science Reviews*, 30(21–22), 3109–3123. <https://doi.org/10.1016/j.quascirev.2011.07.010>

965 Weiss, H. (2016). Climate change and cultural evolution across the world. *Past Global Change Magazine*, 24(2),
966 62–63. <https://doi.org/10.22498/pages.24.2.55>

967 Weiss, H. (2019). Interactive comment on “ Is there evidence for a 4 . 2 ka BP event in the northern North Atlantic
968 region ?” by Raymond Bradley and Jostein Bakke. *Climate of the Past Discussions*.
969 <https://doi.org/https://doi.org/10.5194/cp-2018-162-RC2>, 2019

970 Whitlock, C., & Bartlein, P. J. (1993). Spatial Variations of Holocene Climatic Change in the Yellowstone Region.
971 *Quaternary Research*, 39, 231–238.

972 Wise, E. K. (2010). Spatiotemporal variability of the precipitation dipole transition zone in the western United
973 States. *Geophysical Research Letters*, 37(7), n/a-n/a. <https://doi.org/10.1029/2009gl042193>

974 Xiao, J., Zhang, S., Fan, J., Wen, R., Zhai, D., Tian, Z., & Jiang, D. (2018). The 4.2 ka BP event:
975 Multi-proxy records from a closed lake in the northern margin of the East Asian summer monsoon. *Climate of*
976 *the Past*, 14(10), 1417–1425. <https://doi.org/10.5194/cp-14-1417-2018>

977 Yan, M., & Liu, J. (2019). Physical processes of cooling and mega-drought during the 4.2 ka BP event: Results from
978 TraCE-21ka simulations. *Climate of the Past*, 15(1), 265–277. <https://doi.org/10.5194/cp-15-265-2019>

979 Zhang, H., Cheng, H., Cai, Y., Spötl, C., Kathayat, G., Sinha, A., et al. (2018). Hydroclimatic variations in
980 southeastern China during the 4.2 ka event reflected by stalagmite records. *Climate of the Past*,
981 14(11), 1805–1817. <https://doi.org/10.5194/cp-14-1805-2018>

982 Zhu, C., Lettenmaier, D. P., & Cavazos, T. (2005). Role of antecedent land surface conditions on North American
983 monsoon rainfall variability. *Journal of Climate*, 18(16), 3104-3121. <https://doi.org/10.1175/JCLI3387.1>

984